DNA REPAIR

K63-linked polyubiquitin chains bind to DNA to facilitate DNA damage repair

Pengda Liu[1,2*†], Wenjian Gan[1*], Siyuan Su[2*], Arthur V. Hauenstein[3], Tian-min Fu[3], Bradley Brasher[4], Carsten Schwerdtfeger[4], Anthony C. Liang[5], Ming Xu[6,7], Wenyi Wei[1†]

Polyubiquitylation is canonically viewed as a posttranslational modification that governs protein stability or protein-protein interactions, in which distinct polyubiquitin linkages ultimately determine the fate of modified protein(s). We explored whether polyubiquitin chains have any nonprotein-related function. Using in vitro pull-down assays with synthetic materials, we found that polyubiquitin chains with the Lys[63] (K63) linkage bound to DNA through a motif we called the "DNA-interacting patch" (DIP), which is composed of the adjacent residues Thr[9], Lys[11], and Glu[34]. Upon DNA damage, the binding of K63-linked polyubiquitin chains to DNA enhanced the recruitment of repair factors through their interaction with an Ile[44] patch in ubiquitin to facilitate DNA repair. Furthermore, experimental or cancer patient–derived mutations within the DIP impaired the DNA binding capacity of ubiquitin and subsequently attenuated K63-linked polyubiquitin chain accumulation at sites of DNA damage, thereby resulting in defective DNA repair and increased cellular sensitivity to DNA-damaging agents. Our results therefore highlight a critical physiological role for K63-linked polyubiquitin chains in binding to DNA to facilitate DNA damage repair.

INTRODUCTION

DNA damage is lethal to cells if not repaired properly (*1*) and leads to tumorigenic genomic instability if not repaired accurately and efficiently (*2*). Thus, multiple DNA damage sensing and repair mechanisms have evolved to maintain genome stability (*3*–*5*). The most well-studied DNA damage response (DDR) pathways involve those that respond to DNA double-strand breaks (DSBs) and are initiated by activation of the kinase ataxia-telangiectasia mutated to trigger phosphorylation of H2A histone family, member X (H2Ax) and mediator of DNA damage protein 1, serving to recruit E3 ubiquitin ligases including ring finger protein 8 (RNF8) and RNF168 for a second wave of chromatin modifications. This in turn promotes Lys[63] (K63)–linked polyubiquitination of histones (*6*, *7*), leading to the recruitment of various repair factors, such as the receptor-associated protein 80 (Rap80), to sites of DNA damage to direct homologous recombination (HR) (*8*). In addition, RNF168 also promotes loading of p53-binding protein 1 (53BP1) onto sites of damaged DNA in large part through creating a histone H2A-Lys[15] (K15) ubiquitination mark that is necessary for 53BP1 recognition of chromatin (*9*). Notably, K63-linked polyubiquitin chains accumulate at DSB sites, loss of which leads to deficient DNA damage repair (*10*), supporting a critical role for K63-linked ubiquitin chains in facilitating the repair of damaged DNA. However, thus far, ubiquitination has only been considered a protein modification to govern protein degradation or protein-protein interactions; we were curious whether and how polyubiquitin chains exert any nonprotein-related function.

Given that different linkages of polyubiquitin chains exert distinct cellular functions in vivo, the topologies for several linkages of polyubiquitin chains have been determined to provide structural insights into how each linkage may associate with different signaling features (*11*). Specifically, the protein degradation–oriented K48-linked (*12*) or K11-linked (*13*) polyubiquitin chains adopt compact helical structures (*14*), and K29-linked or K33-linked chains display zigzagging arrays (*15*, *16*), whereas linear or K63-linked polyubiquitin chains exhibit a relatively relaxed and labile structure (*14*, *17*). Thus, it appears that the folding architecture of different polyubiquitin chains may generate versatile signals to govern the fates of modified proteins. Given the relatively labile and extended conformational feature of the structural topology for K63-linked polyubiquitin chains, which mirrors DNA double strands (*11*), it is tempting to postulate that K63-linked polyubiquitin chains might directly bind DNA independent of its canonical role through mediating protein-protein interactions (*8*). Here, we found a previously unknown physiological function for the K63-linked polyubiquitin chains in directly binding DNA to facilitate DNA repair and that mutations in ubiquitin found in cancer patients may facilitate tumorigenesis through impairing this process.

RESULTS

K63-linked polyubiquitin chains bind DNA in vitro

To examine a possible interaction between DNA and polyubiquitin chains, we observed that only the labile K63-linked (Fig. 1A and fig. S1A) but not the structurally compact K48-linked (Fig. 1B and fig. S1B) nor K11-linked (Fig. 1C) polyubiquitin chains interacted with 70-mer double-stranded DNA (dsDNA) or single-stranded DNA (ssDNA) with a random DNA sequence used in a previous study (*18*) in vitro. Notably, linearly linked polyubiquitin chains displayed minimal binding to DNA in vitro, compared with the same lengths of the K63-linked polyubiquitin chains (Fig. 1D and fig. S1, C to E), indicating that it is not the labile topology per se but rather specific

[1]Department of Pathology, Beth Israel Deaconess Medical Center, Harvard Medical School, Boston, MA 02115, USA. [2]Department of Biochemistry and Biophysics, Lineberger Comprehensive Cancer Center, University of North Carolina at Chapel Hill, Chapel Hill, NC 27599, USA. [3]Department of Biological Chemistry and Molecular Pharmacology, Harvard Medical School, and Program in Cellular and Molecular Medicine, Boston Children's Hospital, Boston, MA 02115, USA. [4]Boston Biochem Inc., Cambridge, MA 02139, USA. [5]Department of Genetics and Howard Hughes Medical Institute, Division of Genetics, Brigham and Women's Hospital, Harvard University Medical School, Boston, MA 02115, USA. [6]Department of Molecular Biology, University of Texas Southwestern Medical Center, Dallas, TX 75390, USA. [7]Howard Hughes Medical Institute, University of Texas Southwestern Medical Center, Dallas, TX 75390, USA.
*These authors contributed equally to this work.
†Corresponding author. Email: pengda_liu@med.unc.edu (P.L.); wwei2@bidmc.harvard.edu (W.W.)

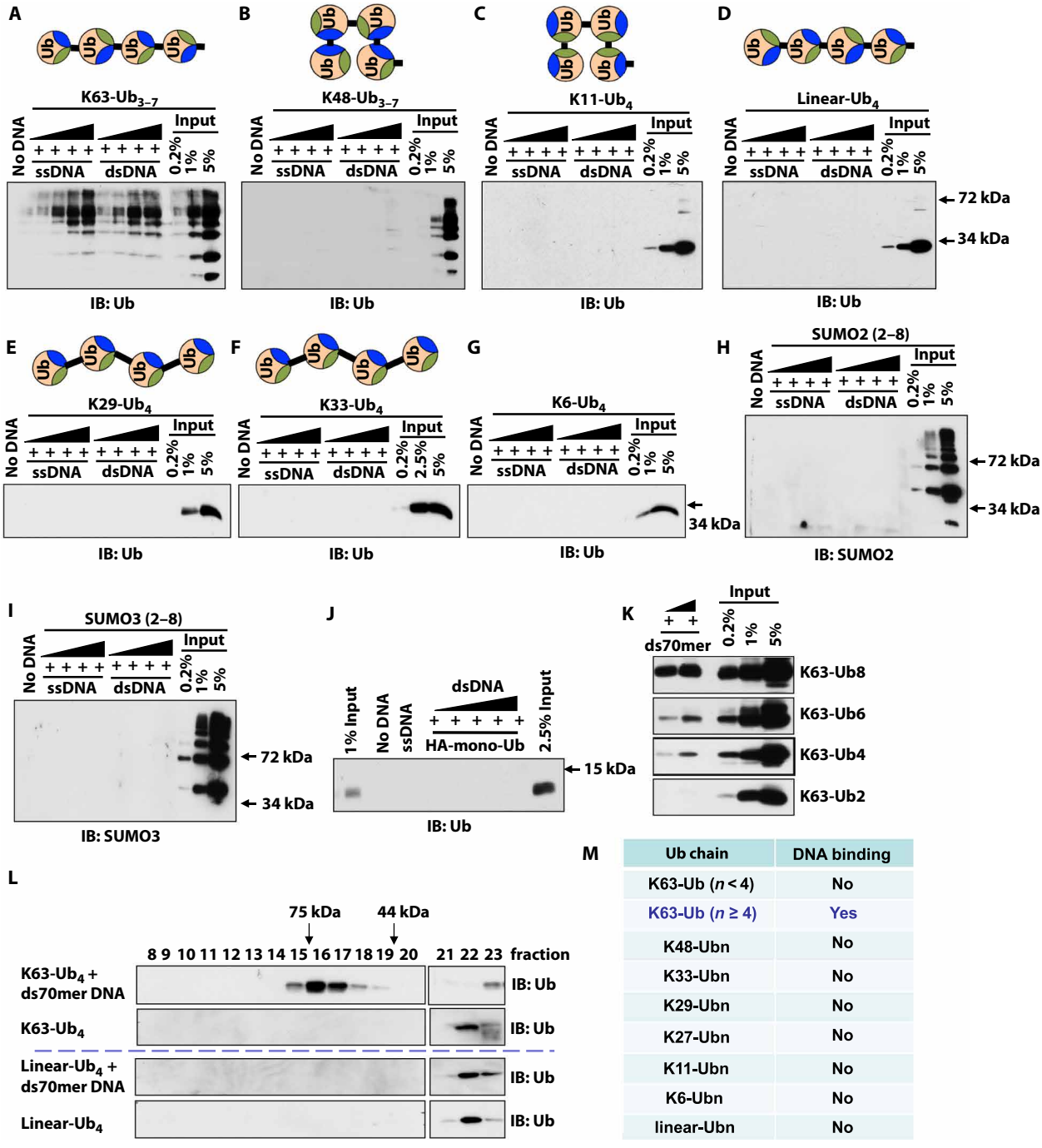

M

Ub chain	DNA binding
K63-Ub ($n < 4$)	No
K63-Ub ($n \geq 4$)	Yes
K48-Ubn	No
K33-Ubn	No
K29-Ubn	No
K27-Ubn	No
K11-Ubn	No
K6-Ubn	No
linear-Ubn	No

Fig. 1. K63-linked polyubiquitin chains interact with DNA in a chain length–dependent manner in vitro. (**A** to **G**) In vitro DNA binding assays for synthetic K63-linked (A), K48-linked (B), K11-linked (C), linearly linked (or M1-linked) (D), K29-linked (E), K33-linked (F), or K6-linked (G) ubiquitin chains. Shown are the subsequent immunoblotting (IB) analyses of biotin–double-stranded 70-mer (ds70mer) or biotin–single-stranded 70-nt (ss70nt) DNA pull-down assays with increasing amounts of synthetic ubiquitin chains. The topologies of ubiquitin chains ($Ub_{3–7}$ or Ub_4) with indicated linkages are presented on top of the blots. Green represents the Ile^{36} patch, and blue represents the Ile^{44} patch. Blots are representative of two experiments. (**H** and **I**) IB analyses of biotin-ds70mer or biotin-ss70nt DNA pull-down assays with indicated synthetic SUMOylation chains. Blots are representative of two experiments. (**J**) IB analyses of biotin-ds70mer or biotin-ss70nt DNA pull-down assays with indicated human influenza hemagglutinin (HA)–tagged synthetic monoubiquitin. Blots are representative of two experiments. (**K**) IB analyses of biotin-ds70mer DNA pull-down assays using each synthetic K63-linked ubiquitin chains with a fixed length as indicated. Blots are representative of two experiments. (**L**) IB analyses of gel filtration chromatography assays with synthetic tetra-ubiquitin chains of the indicated linkages in the presence or absence of ds70mer DNA. Assay used the Superdex 75 column in DNA binding buffers; conalbumin indicates the 75-kDa position, and ovalbumin (chicken) marks 44 kDa. Blots are representative of two experiments. (**M**) A summary table indicating that K63-linked chains of four or more ubiquitin molecules (*n*), but not other linkages of polyubiquitin chains examined, bind DNA in vitro. We could not examine whether $K27-Ub_4$ chains bind DNA.

structural constraint(s) unique to the K63 linkage that confers its specific interaction with DNA. In further support of this notion, we found that the zigzagging K29-linked or K33-linked polyubiquitin chains also did not exhibit binding to DNA (Fig. 1, E and F) nor did the K6-linked polyubiquitin chains with undetermined topology (Fig. 1G). Moreover, poly-SUMO (small ubiquitin-like modifier) chains, although sharing similar conformation with polyubiquitin chains (*19*), displayed almost no affinity to DNA in vitro (Fig. 1, H and I), further highlighting the specificity for the K63-linked polyubiquitin chains in binding DNA.

Notably, the length of DNA over 15 base pair (bp) did not significantly affect its affinity to K63-linked polyubiquitin chains, whereas ssDNA was slightly preferred to dsDNA (fig. S1F). In addition, higher guanine-cytosine content was also relatively preferred in this experimental condition (fig. S1, G and H), suggesting that the major grooves in dsDNA may be involved in binding K63-linked polyubiquitin chains. No significant DNA interaction with monoubiquitin molecules was observed in our experimental conditions (Fig. 1J and fig. S1I), indicating that a single ubiquitin molecule itself is not sufficient to bind DNA. In keeping with this result, K63-linked polyubiquitin chains interacted with DNA in a ubiquitin chain length–dependent manner, where a detectable binding was observed between DNA and polyubiquitin chains containing four or more ubiquitin molecules (Fig. 1K). Consistently, K63-linked but not linear linkage of tetra-ubiquitin chains formed a stable complex with DNA in vitro (Fig. 1, L and M, and fig. S1J). Although each ubiquitin molecule may contain a weak binding motif for DNA (fig. S1I), increasing copies of ubiquitin molecules in the K63-linked polyubiquitin chain may enhance binding to DNA in a cooperative manner (Fig. 1, A and K). Similarly, this synergistic effect has been previously observed in multiple ubiquitin-interacting motifs (UIMs) within ubiquitin-interacting protein(s) (*20*, *21*). In addition, the binding of K63-linked ubiquitin chains to DNA may occur under physiological conditions that are found to be sensitive to salt concentrations (fig. S1, K and L).

In addition, because there are no K27-linked tetra-ubiquitin chains available, and polyubiquitin chains with a length longer than tetra-ubiquitin in linkages other than K63 and K48 have not been successfully synthesized, these technical barriers limit our ability to determine whether non-K63–linked polyubiquitin chains may also bind DNA when formed into longer polyubiquitin chains. To further examine the specificity of K63-linked ubiquitin chains in binding DNA, we found that poly–adenosine 5′-diphosphate–ribose (PAR), another form of physiologically functional and negatively charged polymer in cells (*22*), did not bind K63-linked polyubiquitin chains in vitro (fig. S1M), suggesting that K63-linked ubiquitin chains selectively bind negatively charged polymers including DNA. We also observed that K63-linked ubiquitin chains pulled down nucleosomes purified from HeLa nuclear extracts (fig. S1N) and interacted with in vitro reconstituted, intact nucleosomes containing DNA (fig. S1O) but not histone octamers without DNA (fig. S1, O and P). These data indicate that the observed ubiquitin binding to DNA may be permissive to nucleosomal DNA. However, we cannot rule out the possibility that K63-linked ubiquitin chains bind to chromatin-associated, nonhistone DNA binding proteins, which warrants further investigation. Moreover, K63-linked polyubiquitin chains displayed preference to linear, not circular, DNA in vitro (fig. S1Q). Blocking the free DNA ends reduced DNA recognition by K63-linked ubiquitin chains (fig. S1R). These data suggest that free DNA ends may be necessary to facilitate its binding to ubiquitin chains.

K63-linked polyubiquitin chains interact with DNA via the DIP motif composed of Thr^{9}, Lys^{11}, and Glu^{34} residues in ubiquitin

Given that the Ile^{44} hydrophobic patch in the ubiquitin molecule has been well characterized as the protein-binding module (*23*), next, we went on to examine whether a similar DNA binding patch is present in the ubiquitin molecule. Previous reports have revealed that the E3 ubiquitin ligase tumor necrosis factor receptor-associated factor 6 (TRAF6) (*24*–*26*) and DNA-damaging agents (*27*) can promote the formation of K63-linked polyubiquitin chains in cells. Upon either expressing wild-type TRAF6 (fig. S2A) or treating cells with various chemotherapeutic DNA-damaging drugs, including etoposide, doxorubicin, or cisplatin (Fig. 2A), we observed a significantly enhanced DNA interaction with ubiquitin chains (presumably K63-linked) from cells. These results further indicate that DNA-mediated pull-down of K63-linked polyubiquitin chains recovered from cell lysates could serve as a tool to further dissect the potential DNA binding patch in the ubiquitin molecule.

Using this experimental system, we found that, in keeping with results obtained using purified synthetic polyubiquitin chains in vitro that demonstrate a specific interaction between DNA and K63-linked polyubiquitin chains (Fig. 1, A and K), a ds70mer DNA largely lost its ability to bind polyubiquitin chains composed of the K63R mutant form of ubiquitin that abolishes the synthesis of K63-linked ubiquitin chains (Fig. 2B). Furthermore, similar to those containing the K63R mutation, polyubiquitin chains containing the K11R but not the I44A (Fig. 2B) nor the K48R (fig. S2B) mutation were deficient in binding DNA, indicating that either the K11 linkage or the K11 residue is critical for the interaction between ubiquitin chains and DNA. Polyubiquitin chains composed of the K63-only mutant also displayed a sharp reduction in its affinity to DNA (Fig. 2, C and D), supporting a model that certain side-chain lysine(s) in addition to K63 may be involved in mediating the DNA-ubiquitin interaction. Given that K11 and K48 structurally reside on opposite sides of a ubiquitin molecule in K63-linked polyubiquitin chains (*11*), we restored the K11 residue (designated as "K63/K11") or the K48 residue (designated as "K63/K48") in K63-only mutant containing polyubiquitin chains and reexamined their impact on DNA binding. Notably, restoration of the K11 residue largely rescued the binding of K63/K11 polyubiquitin chains to DNA, whereas adding back the K48 residue only minimally improved its DNA binding affinity (Fig. 2, D and E, and fig. S2C). These results together indicate that, in addition to the requirement of the K63 linkage (the K63 residue), the K11 residue is also indispensable for ubiquitin's interaction with DNA.

To exclude a possible role of K11 linkage in mediating ubiquitin's binding to DNA, we explored the reported crystal structure of K63-linked di-ubiquitin molecules (PDB: 3H7P) (*28*) and, using PyMOL software, identified Thr^{9}, Thr^{12}, Thr^{14}, and Glu^{34} as major residues spatially surrounding Lys^{11} on the ubiquitin surface (Fig. 2F). Notably, similar to the K11R mutant, alanine substitution mutations of either Thr^{9} or Glu^{34}, but not Thr^{12} nor Thr^{14}, significantly reduced ubiquitin's binding affinity to DNA (Fig. 2, G and H). Furthermore, neither T9A nor E34A mutants were deficient in forming polyubiquitin chains (Fig. 2, G and H) or promoting polyubiquitylation of H2Ax by RNF168 (fig. S2D) in cells, thereby excluding the possibility that the loss of binding of these mutated polyubiquitin chains to DNA is due to impaired polyubiquitin chain formation. Together, these data suggest that K63-linked, but not K11-linked, polyubiquitin chains specifically interact with DNA, in large part through the Thr^{9}, Lys^{11}, Glu^{34} residues.

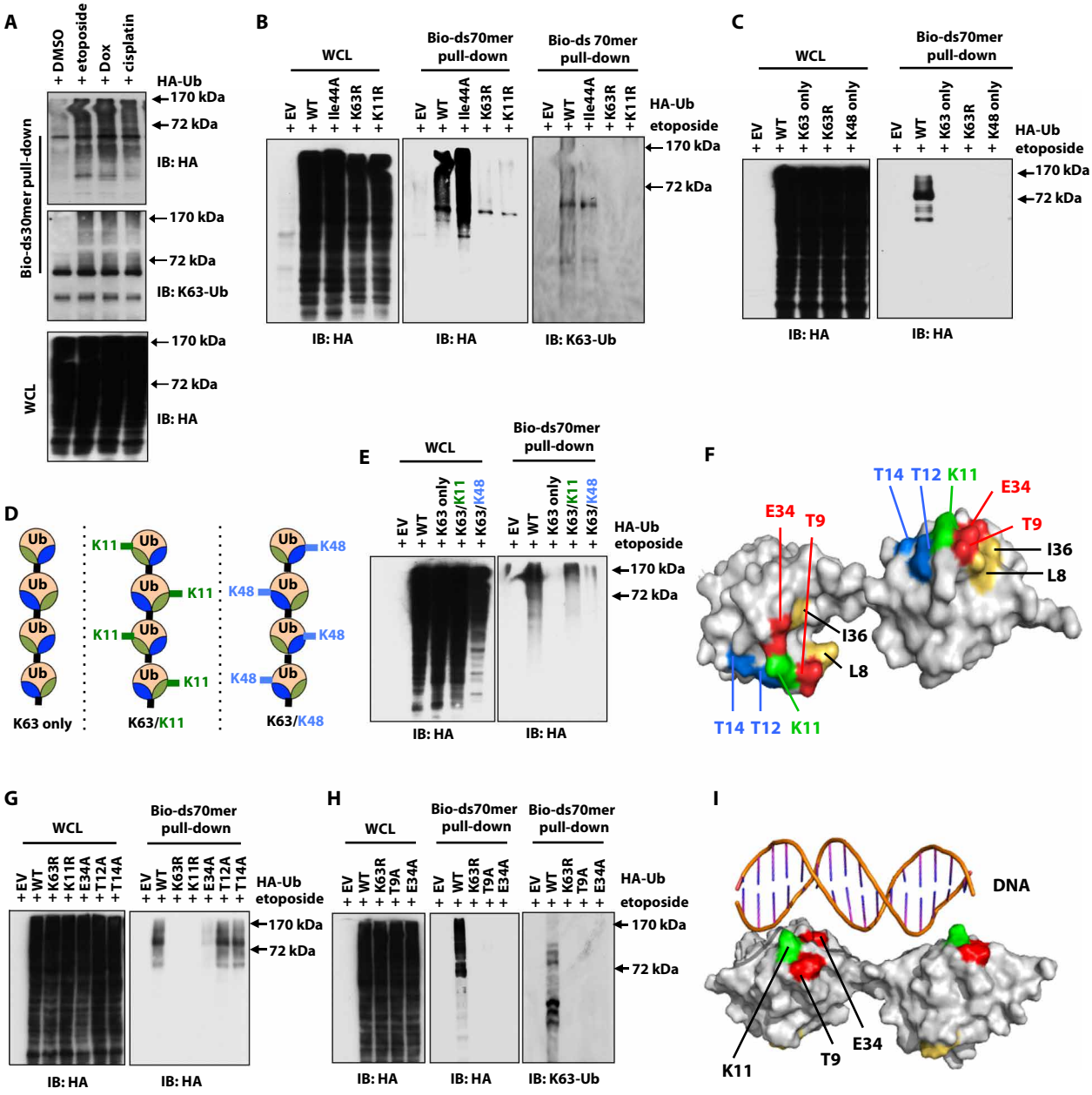

Fig. 2. K63-linked polyubiquitin chains interact with DNA through a DIP motif composed of adjacent Thr^{9}, Lys^{11}, and Glu^{34} residues. (**A**) IB analysis of ds30mer DNA pull-down assays from whole cell lysates (WCL) derived from human embryonic kidney (HEK) 293T cells transfected with HA-ubiquitin and treated with dimethyl sulfoxide (DMSO), etoposide (100 μM), doxorubicin (Dox; 10 μM), or cisplatin (20 μM) for 1 hour before harvesting and incubation with ds30mer DNA. Blots are representative of three experiments. (**B** to **E**) IB analyses of biotin-ds70mer DNA pull-down assays with WCLs derived from HEK293T cells that had been transfected with the indicated HA-tagged ubiquitin construct or empty vector (EV) control and treated with etoposide (20 μM) for 1 hour. Schematics of the structures of K63-only, K63/K11-only (K63/K11), and K63/K48-only (K63/K48) mutant polyubiquitin tested in (E) are presented in (D). Notably, EV represents empty vector as a negative control. Blots are representative of two experiments. WT, wild type. (**F**) Schematic of the location of residues spatially surrounding Lys^{11} derived from a crystal structure [Protein Data Bank (PDB: 3H7P)] of K63-diUb using the PyMOL Molecular Graphics System. Notably, the Lys^{11} residue is labeled in green to indicate a dual role of Lys^{11} in binding DNA and forming the K11 linkage, Thr^{9} and Glu^{34} are marked in red to illustrate their possible role involved in binding DNA, Thr^{12} and Thr^{14} are labeled in blue to indicate that they are not DIP residues, while the other "TEK" (threonine, glutamate, lysine) box residues including Leu^{8} and Ile^{36} are marked in yellow. (**G** and **H**) IB analyses of biotin-ds70mer DNA pull-down assays and WCLs derived from HEK293T cells transfected with indicated HA-ubiquitin constructs and treated with 20 μM etoposide for 1 hour before harvesting for the ds70mer DNA pull-down analysis. Blots are representative of two experiments. (**I**) Ubiquitin-DNA interaction model generated using a nuclear magnetic resonance solution structure of K63-linked di-ubiquitin (PDB: 2RR9) with DNA (PDB: 3BSE) using PyMOL.

Given a possible role of this region of ubiquitin in mediating the interaction between K63-linked ubiquitin chains and DNA, we named the DNA-ubiquitin–interacting motif the "DNA-interacting patch" (or "DIP") (Fig. 2I) in echoing the well-characterized Ile^{44} patch that mainly mediates ubiquitin's interaction with proteins (*29*). Notably, all the DIP residues including Thr^{9}, Lys^{11}, and Glu^{34} are conserved

through evolution (fig. S2E). The DIP motif (Thr^{9}, Lys^{11}, and Glu^{34}) that we identified is part of the "TEK" box (composed of Lys^{11}, Lys^{6}, Leu^{8}, Thr^{9}, Glu^{34}, and Ile^{36}) that is required for UBCH10 [ubiquitin-conjugating enzyme E2 C (also known as UBE2C)]–dependent K11-linked polyubiquitin chain formation (*30*). Notably, although mutation of Leu^{8} to alanine (L8A) led to reduced polyubiquitin chain formation in cells, L8A mutation did not abolish the ability of L8A-containing polyubiquitin chains to bind to DNA (fig. S2F), suggesting that these DIP residues are at least involved in two separate biological processes in a polyubiquitin chain linkage-dependent manner: (i) binding DNA in K63-linked polyubiquitin chains and (ii) promoting nucleation of K11-linked polyubiquitin chains for proper anaphase-promoting complex/cyclosome (APC/C) function. In addition, through examining other ubiquitin-like molecules (*31*), a strong conservation of the DIP motif in neural precursor cell expressed, developmentally down-regulated 8 (NEDD8) was observed (fig. S2G), suggesting that K60-linked NEDD8 chains may also bind DNA. However, because mononeddylation rather than polyneddylation is commonly observed (*32*), whether mono-NEDD8 binds DNA warrants further investigation.

DNA, K63-linked polyubiquitin chains, and Rap80 form a ternary complex in vitro and in cells

Provided that the K63-linked polyubiquitin chains are essential in the repair of damaged DNA by serving as a platform to recruit repair factors, such as Rap80, through a Ile^{44} patch in ubiquitin (*8*, *33*, *34*), we next examined whether DNA binding to the DIP motif interferes with Rap80 binding to K63-linked polyubiquitin chains. We observed that DNA-bound, K63-linked polyubiquitin chains retained the ability to bind Rap80 both when translated in vitro (fig. S3A) and when ectopically expressed in cells (Fig. 3A). Furthermore, increasing amounts of DNA did not significantly impair, but rather slightly promoted, the interaction of polyubiquitin chains with Rap80 in vitro (Fig. 3B). Consistent with previous reports (*8*, *33*, *34*), mutating K63 or Ile^{44}, but not K11, in ubiquitin attenuated its interaction with Rap80 (fig. S3B). On the other hand, T9A mutation– or E34A mutation–containing polyubiquitin chains retained their ability to bind Rap80 in cells (Fig. 3C), suggesting that K63-linked polyubiquitin chains interact with DNA and proteins through distinct patches, and DNA binding to the DIP motif may not interfere with Rap80 binding to the Ile^{44} patch.

In keeping with this notion, DNA, K63-linked polyubiquitin chains, and the UIM domains of Rap80 could form a ternary complex in vitro (Fig. 3D and fig. S3, C and D). These results further confirm that, in addition to recruiting repair factors through the Ile^{44} patch (fig. S3E), K63-linked polyubiquitin chains may also directly anchor the damaged DNA broken ends through an interaction mediated by its DIP motif (fig. S3F), thereby forming a ternary complex (Fig. 3E) to cooperatively promote DNA damage repair. Although further investigation is needed to rigorously examine this model, these results indicate that, in addition to recruiting repair proteins to the site of DNA damage, the presence of the K63-linked polyubiquitin chains may also serve to bridge two broken DNA ends to assemble a local repair machinery, thus guiding the spatial repair of the damaged DNA.

DNA binding–deficient ubiquitin mutations attenuate accumulation of K63-linked polyubiquitin chains at the site of DNA damage and sensitize cells to DNA-damaging agents

Genetic evidence has demonstrated a critical role for K63-linked polyubiquitin chains in facilitating DNA damage repair (*35*), in part through recruiting key repair factors (*27*, *36*). To examine whether the DNA binding ability of K63-linked polyubiquitin chains is critical during the DDR, we used the budding yeast as a model system and replaced the endogenous ubiquitin with exogenous wild-type ubiquitin, or DNA binding–deficient ubiquitin mutants (including K63R, K11R) or the DIP motif mutants T9A or E34A, either in a glucose-driven manner (Fig. 4A) or by the standard plasmid shuffle approach (Fig. 4B and fig. S4A). We observed greater sensitivity of K63R-expressing yeast cells [in agreement with a previous report (*35*)] and K11R-expressing yeast cells to various DNA-damaging agents, including methyl methanesulfonate (MMS), etoposide, and camptothecin (CPT) (Fig. 4A and fig. S4B). Notably, no additive sensitivity to these treatments was observed in yeast cells expressing the K11R/K63R double mutant (fig. S4B), suggesting that the K63 and K11 residues largely function to regulate DNA damage repair through the same genetic pathway. Moreover, other atypical linkages, including K6, K27, K29, and K33, also appeared to play pivotal roles in promoting DNA damage repair and cell survival under distinct DNA-damaging conditions with unclear mechanism(s) (fig. S4C). Furthermore, phenocopying the K63R mutant, yeast strains bearing the DIP motif T9A or E34A ubiquitin mutations that disrupt interactions between DNA and K63-linked polyubiquitin chains displayed an increased sensitivity to MMS and bleocin (Fig. 4B and fig. S4D), although this may be in part mediated through K63-linked polyubiquitylation of proliferating cell nuclear antigen (PCNA) (fig. S4E) (*37*, *38*). These results therefore support a critical physiological role for the interaction between DNA and K63-linked polyubiquitin chain in facilitating the DDR and cell survival in yeast.

In support of our findings in yeast, using a mammalian Tet-on system to replace endogenous ubiquitin with the E34A mutant in U2OS cells (fig. S4F) (*39*), we observed that, similar to the K63R mutant, E34A-expressing U2OS cells were deficient in their ability to timely repair ionizing radiation (IR)–damaged DNA, as evidenced by sustained γH2Ax signals (fig. S4, G and H), resulting in greater sensitivity to chemotherapeutic challenges such as bleocin (Fig. 4C), etoposide (Fig. 4D), and doxorubicin (Fig. 4E). These deficiencies are in part due to the failure of the E34A-containing polyubiquitin chains to accumulate at the site of DNA damage (Fig. 4, F and G), which might subsequently lead to imprecise or insufficient loading of key factors to repair damaged DNA. Together, these data support an indispensable role for the interaction of DNA with K63-linked ubiquitin chains to mediate the timely repair of damaged DNA.

DIP mutations in ubiquitin found in patient tumors suppress the binding of K63-linked polyubiquitin chains to DNA

Given that human pathological disorders frequently hijack critical signaling pathways to favor tumorigenesis (*40*), next, we examined whether there are somatic mutations occurring within the ubiquitin DIP motif in human cancer. From the cBioPortal database (www.cbioportal.org), we found two cases of E34K mutations and one case with T9P mutation in the human *UBC* gene in lung cancer, melanoma, and breast cancer patients, respectively (Fig. 5A). Note that, because of the tandem arrangement of multiple copies of ubiquitins in the *UBC* gene, E110K and E186K mutations correspond to Glu^{34} and T617P to Thr^{9} in a single ubiquitin molecule (hence, referred to as E34K and T9P). Both the E34K and T9P mutants displayed significantly decreased binding to DNA (Fig. 5B). Given that binding to DNA requires a length of at least four ubiquitin molecules in K63-linked polyubiquitin chains (Fig. 1K), incorporation of a mutated form of ubiquitin in a tetra-ubiquitin region in a polyubiquitin chain might

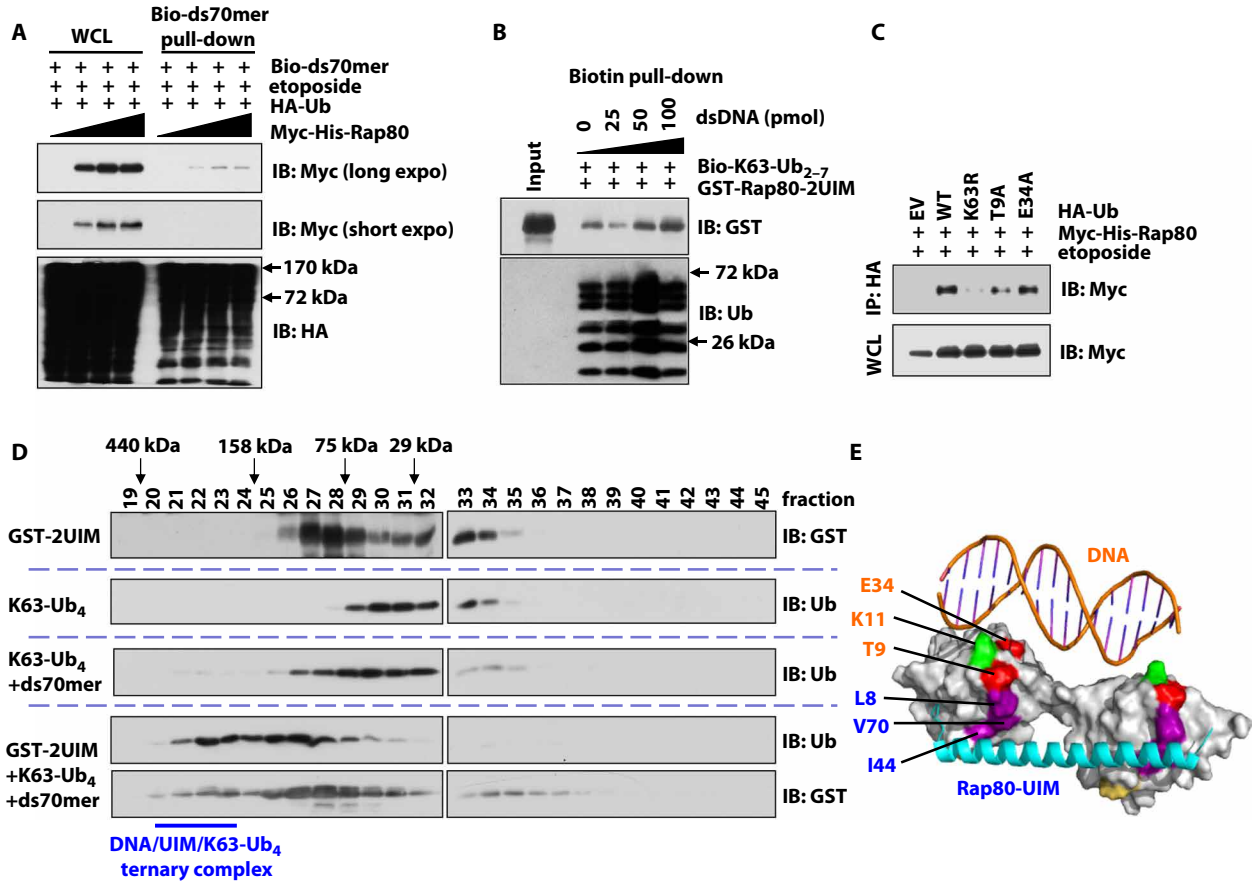

Fig. 3. K63-linked polyubiquitin chains interact with DNA and Rap80 to form a ternary complex. (**A**) IB analysis of biotin-ds70mer DNA pull-downs in WCLs derived from HEK293 cells transfected with HA-ubiquitin and increasing amounts of Myc-His-Rap80 and, 48 hours later, treated with etoposide (20 μM) for 1 hour. Blots are representative of two experiments. (**B**) IB analysis of biotin-K63-Ub_{2-7} chain pull-down products with increasing doses of ds70mer DNA. Blots are representative of two experiments. GST, glutathione *S*-transferase. (**C**) IB of WCLs and HA–immunoprecipitations (IPs) derived from HEK293T cells transfected with indicated constructs and treated with etoposide (20 μM). Blot for HA in the WCL is shown in Fig. 2H. Blots are representative of two experiments. (**D**) Gel filtration analysis of biotin-ds70mer DNA incubated with K63-Ub_4 in the presence or absence of bacterially purified GST-Rap80-2UIM protein at 4°C for 2 hours. (**E**) A computer modeling illustration for a putative complex composed of DNA, K63-linked di-ubiquitin, and the UIM domain of Rap80 using a DNA structure [PDB: 3BSE (*55*)] superimposed onto the solved structure of a K63-linked di-ubiquitin complexed with UIM domains of Rap80 (PDB: 3A1Q).

play a dominant-negative role by disrupting its binding to DNA (Fig. 5C). In support of this notion, ectopic expression of either the T9P or the E34K ubiquitin variants in the presence of wild-type ubiquitin in HEK293T cells resulted in attenuation of polyubiquitin chain binding to DNA (Fig. 5D and fig. S5A).

In MDA-MB-231 and HCT116 cells, expression of T9P- or E34K-mutant ubiquitin impaired DNA damage repair (fig. S5, B and C), evident as sustained foci formation of Rap80 and γH2Ax upon challenge with IR (Fig. 5, E to G). As a consequence, cells expressing T9P ubiquitin were more sensitive to IR (fig. S5, D to G) and etoposide (fig. S5, H and I). Notably, although both the T9P and E34K mutations occur in the TEK box (*41*) as well, the APC/C activity was not significantly affected by these DIP mutations (fig. S5, B and C), suggesting that the observed biological effects caused by T9P or E34K mutant are unlikely to be due to impaired APC/C function. Moreover, although the E34 residue has been shown to interact with the Ring domain of RNF4 (*42*) and breast cancer type 1 susceptibility protein (BRCA1) (*43*), expression of a mutant form of E34K ubiquitin in HEK293T cells displayed minimal effects on ubiquitination of downstream substrates, such as Tax and H2A, in cells by RNF4 (fig. S5J) and BRCA1 (fig. S5K), respectively. These data suggest that, at least in our experimental setting for the substrates that we examined, the deficient DNA damage repair in cells expressing E34K ubiquitin is unlikely to be due to impairment of the E3 ligase activities of either BRCA1 or RNF4.

Hence, these DIP motif mutations led to enhanced sensitivity of U2OS cells to both radiotherapeutic and chemotherapeutic treatments in large part due to attenuated interaction with DNA, in a dominant-negative manner when wild-type ubiquitin is present, largely through modulating the processes of both HR (fig. S5, L and M) and nonhomologous end joining (fig. S5N). Notably, HEK293T cells expressing either T9P or E34K displayed similar sensitivity to non-DNA damage agents, including the BCL-2 (B cell lymphoma 2) inhibitor ABT-737 (fig. S5, O and P) and the antimitotic microtubule-binding agent Taxol (also known as paclitaxel; fig. S5, Q and R), supporting the notion that the DNA binding ability of K63-linked ubiquitin chains may play critical roles in mediating the DDR but not the cellular apoptotic response.

In addition, although both T9P and E34K mutants exhibited deficiency in repairing DNA breaks caused by IR (Fig. 5, E to G),

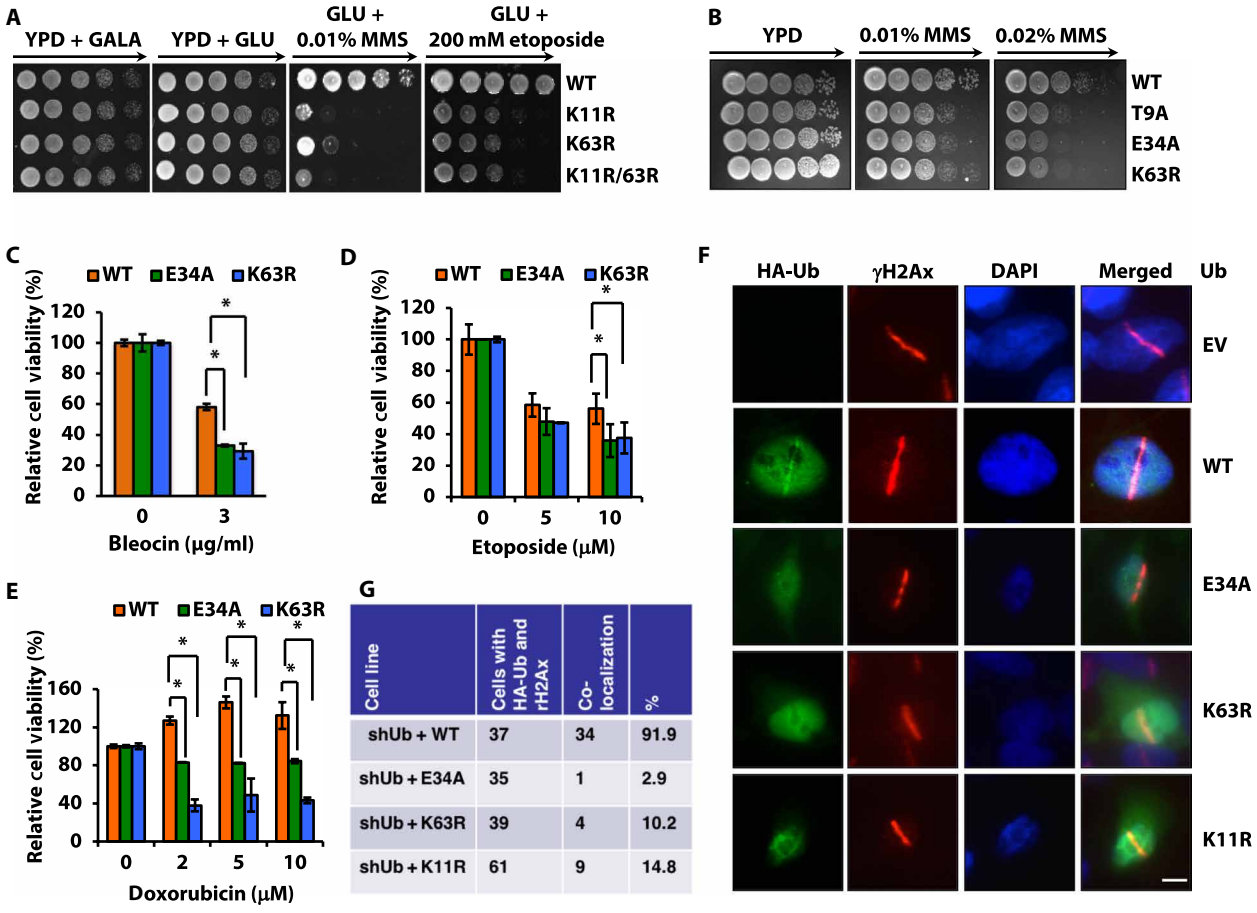

G

Cell line	Cells with HA-Ub and rH2Ax	Co-localization	%
shUb + WT	37	34	91.9
shUb + E34A	35	1	2.9
shUb + K63R	39	4	10.2
shUb + K11R	61	9	14.8

Fig. 4. The binding of DNA to K63-linked polyubiquitin chains is necessary for efficient DNA damage repair. (**A** and **B**) Sensitivity assays in yeast cells expressing the indicated WT or single or double mutant ubiquitin, cultured in YPD (yeast extract-peptone-dextrose) medium with either galactose (GALA) or glucose (GLU) and treated with MMS or etoposide. (**C** to **E**) Cell viability assays in human bone osteosarcoma epithelial U2OS cells transfected with the indicated ubiquitin construct that were cultured with doxycycline (1 μg/ml) for 36 hours and then treated with bleocin (C), etoposide (D), or doxorubicin (E) for another 36 hours. Data are means ± SD from three independent experiments. *$P < 0.05$ by Student's *t* test. (**F** and **G**) Representative images (F) and quantification (G) of HA-tagged ubiquitin (green) colocalization with DNA damage (γH2Ax foci; red) upon laser stripping in U2OS cells in which endogenous ubiquitin had been knocked down and replaced with the indicated WT or mutant construct. Scale bar, 10 μm. DAPI, 4′,6-diamidino-2-phenylindole.

upon ultraviolet (UV) light–induced DNA cross-linking, only cells expressing T9P but not E34K ubiquitins displayed an impaired ability to repair damaged DNA (fig. S5, S and T), suggesting that the role of the DNA binding ability for the K63-linked ubiquitin chains in facilitating DNA damage repair may be DNA damage type–dependent, which also warrants further characterization to reveal the underlying molecular mechanisms.

DISCUSSION

K63-linked polyubiquitylation is essential for DNA damage repair (*44*), inflammation, and the immune response (*45*, *46*) by either serving as a protein posttranslational modification or interacting with distinct subsets of protein factors. Here, we identify that, independent of its canonical protein-related roles, K63-linked ubiquitin chains interacted with DNA in a ubiquitin chain length–dependent manner and through a DIP region in ubiquitin that critically includes Thr^{9}, Lys^{11}, and Glu^{34}. Notably, this identified DIP motif localizes spatially distant from the Ile^{44} patch that mediates the interaction of K63-linked ubiquitin chains with Rap80, indicating that the DNA binding and the protein-binding function of the K63-linked polyubiquitin chains could contribute synergistically to govern DNA damage repair.

Further insights from the structure view of the ternary complex of K63-linked polyubiquitin chains, DNA, and Rap80 would provide detailed molecular mechanisms for the synergistic role of polyubiquitin chains in binding both DNA and proteins simultaneously. However, we also recognize that, because of technical challenges, we cannot fully exclude the possibility that mutating the DIP motif may also interfere with the binding of K63-linked polyubiquitin chains to deubiquitinases that could modulate ubiquitin chain formation, or certain DNA damage repair factors rather than Rap80, which warrants further investigation. Furthermore, this manuscript mainly focuses on examining the features of ubiquitin in binding nucleotides, and the specificity contributed by DNA sequence/motifs in the DNA-ubiquitin interactions remains to be further determined.

A growing body of literature is beginning to establish a ubiquitin code where the "builders" (namely, E2 and E3 ubiquitin ligases that synthesize polyubiquitin chains via various linkages) and "readers"

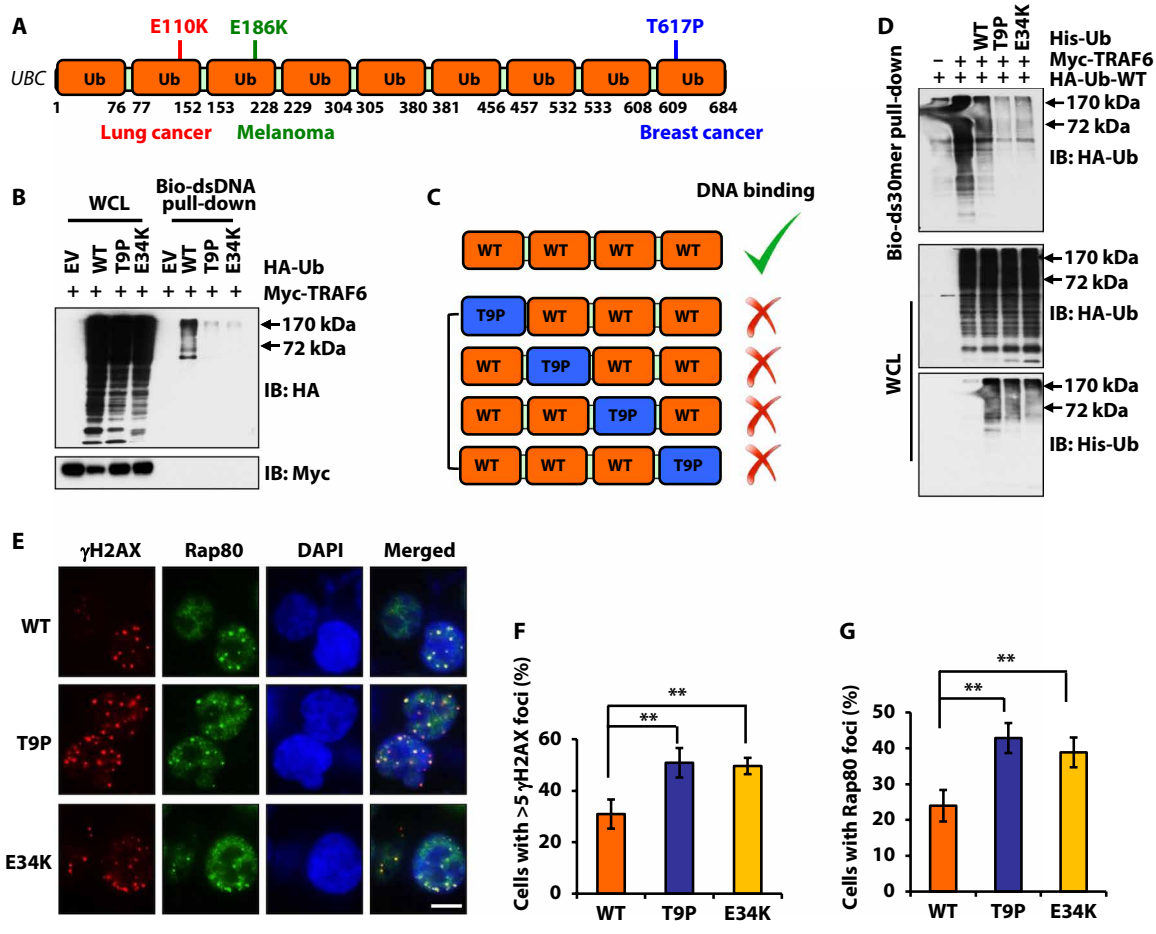

Fig. 5. T9P or E34K ubiquitin mutants observed in cancer patients suppress the binding of K63-linked polyubiquitin chains to DNA. (**A**) Schematic of the patient tumor–derived ubiquitin mutations in *UBC* (*UBC* is a polyubiquitin gene in which E110K/E186K and T617P correspond to E34K and T9P in the ubiquitin protein), obtained from the cBioPortal database. Ub, monoubiquitin. (**B**) IB analysis of WCL and biotin-ds30mer DNA pull-downs derived from HEK293T cells transfected with the indicated construct of ubiquitin (EV) and Myc-tagged TRAF6. Blots are representative of two experiments. (**C**) Schematic of the proposed dominant-negative function of the mutated ubiquitin gene. If a mutant ubiquitin is present in any of four links of the ubiquitin chain, then it will lead to abolished DNA binding of the tetra-ubiquitin region. (**D**) IB analysis of WCL and biotin-ds30mer DNA pull-downs derived from HEK293T cells transfected with WT, HA-tagged ubiquitin (HA-Ub-WT), Myc-TRAF6, and the indicated additional WT or mutant ubiquitin construct. Blots are representative of two experiments. (**E** to **G**) Representative images (E) and quantification (F and G) of HCT116 cells stably expressing the indicated ubiquitin constructs exposed to 5-gray IR and recovered for 24 hours and then stained with antibodies against the indicated molecules. At least 100 cells were analyzed for each group. Data are means ± SD from three independent experiments. $^{**}P < 0.01$ by Student's *t* test. Scale bar, 10 μm.

(referring to ubiquitin-binding proteins that carry out distinct cellular functions to decipher the ubiquitin chain linkage information), as well as the topology and physiological function of different atypical linkage polyubiquitin chains, combine to dictate cellular responses to various stimuli. However, the resolution of the map for the "ubiquitin code" is still relatively low. To this end, it remains unknown, in addition to K63-linked, whether K27-linked polyubiquitin chains are able to bind DNA and whether this binding capacity is critical for their physiological function because of the technical difficulty in synthesizing K27-linked polyubiquitin chains in vitro.

Our data also suggest that K63-linked polyubiquitin chains interact with DNA to modulate the DDR. Thus, we speculate that poly–K63-linked ubiquitin chains might also interact with naked polynucleotides in other cellular contexts such as DNA replication forks and surveillance of viral infection to actively participate in various cellular processes. Distinct from poly-sumoylation chains that do not bind DNA but actively participate in the immune response and host-pathogen defense (*47*), K63-linked polyubiquitin chains may in part serve as a layer of the immune system by serving as a sponge for cytoplasmic foreign DNA from viral or bacterial infections, which warrants further in-depth investigation.

MATERIALS AND METHODS

Cell culture

HEK293T, HEK293, HCT116, MDA-MB-231, and U2OS cells routinely used in the laboratory or requested from collaborators were maintained in Dulbecco's modified Eagle's medium (DMEM) supplemented with 10% fetal bovine serum, 100 U of penicillin, and streptomycin (100 μg/ml). No mycoplasma contamination was observed.

Cell transfection was performed using Lipofectamine and plus reagents (#18324-012, Life Technologies) or Lipofectamine LTX reagents (#15338100, Life Technologies), as described previously (*48*–*50*). Packaging of various lentiviral pLenti-HA-ubiquitin viruses and retroviral pBabe-HA-ubiquitin–expressing viruses and subsequent infection of various cell lines were performed according to the protocol described previously (*48*). Etoposide (E1383), doxorubicin (D1515), hydroxyurea (H8627), CPT (C9911), 5-fluorouracil (F6627), and doxocycline (D9891) were purchased from Sigma. Cisplatin (S1166) was purchased from Selleck Chemicals. Bleocin (203408) was purchased from Calbiochem. MMS (156890250) was purchased from Thermo Fisher Scientific Acros Organics.

Plasmids

Myc-TRAF6-WT and Myc-TRAF6-C70A were obtained from Y. Sun (University of Michigan). pcDNA3-HA-ubiquitin-WT was generated in the laboratory by cloning the human *UBC* complementary DNAs (cDNAs) into pCDNA3-HA vector via BamHI and XhoI sites. pcDNA3-super-His-ubiquitin-WT was generated by cloning the human *UBC* cDNAs into pcDNA3 vector via BamHI and XhoI sites with 6×Histidine tag designed in the forward primer sequence. The corresponding HA-ubiquitin-K63R, K48R, K11R, T9A, T9P, T12A, T14A, E34A, or E34K mutants, as well as pSuper-His-ubiquitin-T9A or E34A, were generated with mutagenesis primers using the QuikChange XL Site-Directed Mutagenesis Kit (Stratagene) according to the manufacturer's instructions. HA-ub-K63–only, K48-only, and K0 plasmids were obtained from the laboratory of V. Poojary (Baylor Institute for Immunology Research). The Flag-HA-BRCA1 plasmid was a gift from G. Gupta (University of North Carolina at Chapel Hill). The H2A plasmid was purchased from transOMIC technologies and subsequently subcloned into pcDNA3-HA vector using BglII/BamHI and XhoI sites. pBabe-HA-Tax was as described (*51*). The RNF4 cDNA was purchased from Addgene (59743) and subcloned into CMV-GST vector using BamHI/SalI sites. More details of plasmid constructions will be provided upon request.

Antibodies

All antibodies were used at a 1:1000 dilution in 5% nonfat milk for Western blotting. Antibodies to ubiquitin (catalog no. 3936), SUMO 2/3 (4971), phospho-S473-AKT (4060), AKT1 (2938), K63 linkage–specific polyubiquitin (5621), Myc-Tag (polyclonal; 2278), Myc-Tag (monoclonal; 2276), pS139-H2Ax (9718), H3 (4499), and horseradish peroxidase–conjugated biotin (7075) were purchased from Cell Signaling Technology. Antibodies to polyclonal cyclin A2 (polyclonal; catalog no. sc-751), CDH1 (monoclonal; sc-56312), cyclin B1 (polyclonal; sc-594), Cdc20 (monoclonal; sc-13162), HA (polyclonal; sc-805), and GST (polyclonal; sc-459) were purchased from Santa Cruz Biotechnology. Antibodies to tubulin (T-5168), Flag (polyclonal; F-2425), Flag (monoclonal; F-3165, clone M2), Flag agarose beads (A-2220), and HA agarose beads (A-2095), as well as horseradish peroxidase–conjugated anti-mouse secondary antibody (A-4416) and horseradish peroxidase–conjugated anti-rabbit secondary antibody (A-4914), were purchased from Sigma. Monoclonal antibody to HA (901502) was purchased from BioLegend. Antibodies used for immunofluorescent microscopy work were used at the indicated dilution with 1% bovine serum albumin (BSA) [γH2Ax (1:400), Rap80 (1:250), and HA (1:250)] and incubated at room temperature. Antibody to pSer^{139}-H2Ax (monoclonal, raised in mouse; 05-636) was purchased from Millipore. Antibody to Rap80 (monoclonal, raised in rabbit; ab124763) was purchased from Abcam. Antibody to 53BP1 (monoclonal, raised in mouse; 612522) was purchased from BD Biosciences. Antibody to HA (monoclonal, raised in mouse; 901502) was purchased from BioLegend.

Immunoblots and immunoprecipitation

Cells were lysed in EBC buffer [50 mM tris (pH 7.5), 120 mM NaCl, and 0.5% NP-40] supplemented with protease inhibitors (cOmplete Mini, Roche) and phosphatase inhibitors (phosphatase inhibitor cocktail sets I and II, Calbiochem). The protein concentrations of lysates were measured by the Beckman Coulter DU-800 spectrophotometer using the Bio-Rad protein assay reagent. Same amounts of WCLs were resolved by SDS–polyacrylamide gel electrophoresis (PAGE) and immunoblotted with indicated antibodies. For immunoprecipitation, 1000 μg of lysates was incubated with 50% slurry of the indicated affinity gel for 4 hours or the indicated antibody (1 to 2 μg) for 3 to 4 hours, followed by 1-hour incubation with Protein A sepharose beads (GE Healthcare) at 4°C. Immunoprecipitates were washed four times with NETN buffer [20 mM tris (pH 8.0), 100 mM NaCl, 1 mM EDTA, and 0.5% NP-40) before being resolved by SDS-PAGE and immunoblotted with indicated antibodies.

DNA oligonucleotides

To generate DNA structures with dsDNA regions, equal moles of the complimentary DNA oligonucleotides were annealed. The sequences of the DNA oligonucleotides used in this study are random sequence as described previously (*18*) and listed in table S1.

DNA binding assays

For each binding reaction, 200 μl of 0.5 μM biotin-DNA (synthesized by Integrated DNA Technologies oligos) was incubated with streptavidin-coated agarose beads (20349, Thermo Fisher Scientific) at room temperature for 1 hour with gentle rotation and washed thoroughly to eliminate excess DNA. Then, the beads coated with DNA were incubated with 1 μg of synthetic ubiquitin peptides (purchased from Boston Biochem Inc.) or 1000 μg of WCLs in the DNA binding buffer [10 mM tris-HCl (pH 7.5), 100 mM NaCl, 10% glycerol, 0.01% NP-40, and BSA (10 mg/ml)] at 4°C for 2 hours and washed thoroughly in the binding buffer before subjected to immunoblotting analyses.

Synthetic ubiquitin, SUMO, and PAR chains with various linkages

The following synthetic ubiquitin and SUMO chains used in this study were purchased from Boston Biochem Inc.: wild-type K48-linked polyubiquitin chains (Ub3–7; catalog no. UC-230); wild-type K48-linked tetra-ubiquitin (Ub4; UC-210); K63-linked polyubiquitin chains (Ub3–7; UC-320); K63-linked octa-ubiquitin (Ub8; UC-318); K63-linked hexa-ubiquitin (Ub6; UC-317); wild-type K63-linked tetra-ubiquitin (Ub4; UC-310); K63-linked, wild-type, biotin-tagged polyubiquitin chains (Ub2–7; UCB-330); K48-linked, wild-type, biotin-tagged polyubiquitin (Ub2–7; UCB-230); linear tetra-ubiquitin (Ub4; UC-710); K6-linked, wild-type tetra-ubiquitin (Ub4; UC-15-025); K29-linked, wild-type tetra-ubiquitin (Ub4; UC-103-025); and K11-linked, wild-type poly-SUMO2 and poly-SUMO3 (2 to 8 chains; ULC-210 and ULC-310, respectively). K11-linked tetra-ubiquitin (Ub4) chains were gifts from D. Komander [Medical Research Council (MRC) Laboratory of Molecular Biology]. Linear ubiquitin chains (2 to 11) were purchased from Enzo (BML-UW0825). PAR chains were purchased from Trevigen (4336-100-02).

DNA labeling and autoradiography

The 250-bp dsDNA was obtained from polymerase chain reaction (PCR) products (hAkt1 aa 160-410) and was labeled by γ-^{32}P-ATP at 5′ ends using the T4 polynucleotide kinase (New England BioLabs). Briefly, 10 nmol of DNA was incubated with 50 U of T4 kinase and 20 μCi of γ-^{32}P-ATP at 37°C for 1 hour. Labeled DNA was purified through QIA PCR purification kit (QIAGEN) according to the manufacturer's instruction. Twenty microliters of ^{32}P-labeled DNA was mixed with K63-linked or K48-linked polyubiquitin chains preincubated with biotin-ds70mer or biotin-ss70nt DNA and 8 μl of streptavidin agarose beads. Reactions were terminated by adding SDS sample buffer and digested with proteinase K (2 mg/ml) at 37°C for 1 hour. Samples were then analyzed on 1% tris-acetate-EDTA agarose gel and subjected to autoradiography.

In vitro translation of Rap80 and autoradiography

pcDNA3-Myc-His-Rap80 was used as the template to perform the in vitro translation (IVT) experiment with ^{35}S-Met using the TnT Quick Coupled Transcription/Translation System (Promega) according to the manufacturer's instructions. Two hundred microliters of 0.5 μM biotin-ds70mer DNA was incubated with 1 μg of K63-linked polyubiquitin (2 to 7) chains at room temperature for 2 hours and washed thoroughly to eliminate nonspecific binding. Increased amounts of IVT-Rap80 (10, 20, and 30 μl, respectively) were added and further incubated at 4°C for 2 hours before being washed thoroughly and resolved on SDS-PAGE for autoradiography.

Immunofluorescence analysis

The method was adapted from previous studies as described (*49*, *52*, *53*). Cells were grown on glass coverslips for 24 hours and fixed with 3.7% formaldehyde in 1× phosphate-buffered saline (PBS) for 15 min at room temperature and permeabilized with 0.1% Triton X-100 in 1× PBS for 5 min. Samples were rinsed three times in 1× PBS with 5 min each wash, blocked for 30 min with 5% BSA, and incubated with primary antibodies as indicated for 2 hours. After three 5-min washes in 1× PBS with Tween-20 (PBST) (0.1% Tween 20), the coverslips were incubated with Alexa 488–conjugated goat anti-rabbit secondary antibody or Alexa 594–conjugated goat anti-mouse secondary antibody (Invitrogen) for 60 min and washed three times with 1× PBST. Nuclei were counterstained with 4′,6-diamidino-2-phenylindole for 10 min. Coverslips were washed twice for 3 min each with 1× PBS and mounted onto slides using ProLong Gold anti-fade reagent (Invitrogen). Images were acquired by Nikon NIS Elements 4.0 software using Nikon Eclips Ti.

Gel filtration chromatography analysis

The indicated reaction products were filtered through a 0.2-μm syringe filter and loaded onto a Superdex 200 10/300 GL column (catalog no. 17-5175-01, GE Lifesciences) or a Superdex 75 10/300 GL column (catalog no. 17-5174-01, GE Lifesciences). Specifically, 2 μg of K63-Ub4 (~0.0625 nM), 2 μg of linear Ub4 (~0.0625 nM), 2 μg of K63-Ub6 (~0.04 nM), 0.25 nM ds70mer DNA, 6 μg of GST-Rap80-2UIM (44 kDa, ~0.14 nM), or 6 μg of GST (26 kDa, ~0.34 nM) was used in the gel filtration assays. Molecular weight standards used for the Superdex 75 column are 75 kDa (conalbumin) and 44 kDa (ovalbumin; chicken). Molecular weight standards used for the Superdex 200 column are 669 kDa (thyroglobulin), 440 kDa (ferritin), 158 kDa (aldolase), and 75 kDa (conalbumin). Chromatography was performed on the AKTA-FPLC (catalog no. 18-1900-26, GE Lifesciences) with the DNA binding buffer [10 mM tris-HCl (pH 7.5), 100 mM NaCl, 10% glycerol, 0.01% NP-40, and BSA (10 mg/ml)]. One column volume of elute was fractionated, with 300 μl in each fraction, at the elution speed of 0.5 ml min^{-1}. Thirty microliters of aliquots of each fraction was loaded onto SDS-PAGE gels and detected with indicated antibodies.

Electrophoretic mobility shift assay

A PCR product of the DNA sequence of human AKT1 (aa 409-481) with a size of 216 bp was purified with Qiagen PCR purification kit and labeled with γ-^{32}P-ATP in vitro by T4 polynucleotide kinase (M0201, New England BioLabs) at 37 °C for 30 min with a total volume of 50 μl. The resulting reaction products were quenched, and the nonincorporated radioactive ATPs (adenosine 5′-triphosphates) were removed by micro-spin columns. Two microliters of the resulting labeled DNA was mixed with 2 μl of indicated polyubiquitin chains (for K63-Ub_6: 0.25, 0.5, and 1 μg/μl; for linear-Ub_6: 0.5 and 1 μg/μl; for K48-Ub_5: 0.5 and 1 μg/μl) and 5 μl of the master mix (2× DNA binding buffer). Samples were spin down at 5000 rpm for 5 min and incubated at 37°C for 30 min. Then, samples were placed on ice for 5 min before 1 μl of 10× native gel loading buffer was added. All samples were dissolved on 8% native gel, and radioactivity was determined by autoradiography.

Computational modeling

Structures of K63-linked di-ubiquitin alone (Fig. 2F and fig. S3, E and F) with DNA (Fig. 2I) or with both DNA and the Rap80 UIM domain (Fig. 3E) were visualized using the PyMOL Molecular Graphics System. As indicated in the figure legends, PDB entries 3H7P and 2RR9 were used for K63-linked di-ubiquitin, PDB entry 3BSE was used for DNA, and PDB entry 3A1Q was used for Rap80-UIM domain.

IR protocol

Cells were plated 1 day before IR treatment, and the culture dishes (with cells attached) were brought to ionizing radiator with caesium-137 as the irradiated source maintained by Harvard Medical School. Cells were treated with indicated IR doses following the caesium-137 dose guide and then recovered for 1 to 24 hours, as indicated before performing experiments.

cBioportal data analyses

Cancer patient–derived somatic ubiquitin mutations in the *UBC* gene were identified in cBioportal (www.cbioportal.org/) in February 2015. Mutations at either T9 or E34 residues in a single ubiquitin molecule were identified and labeled in Fig. 5A.

HR and non-HR assays in cells

DR-U2OS cell lines with the integrated HR reporter DR-GFP and pCBA-SceI expressing plasmid were provided by S.-Y. Lin (Memorial Sloan-Kettering Cancer Center, New York, NY). Assays were performed as described previously (*53*). Briefly, cells were transfected with pCBA-SceI and, 48 hours later, were subjected to flow cytometry analysis to quantify green fluorescent protein (GFP)–positive cells. Cells were incubated in sodium butyrate (5 mM) for 16 hours to induce chromatin relaxation before analysis by flow cytometry. Genomic DNA was isolated from mock- or I-SceI–transfected cells. PCR was performed using primers CTGCTAACCATGTTCATGCC (DRGFP-F) and AAGTCGTGCTGCTTCATGTG (DRGFP-R). PCR products were digested with I-SceI or I-SceI + BcgI.

Cell viability assays

Cells were plated at 2000 per well in 96-well plates and incubated with complete DMEM containing different concentrations of etoposide (E1383, Sigma), cisplatin (S1166, Selleck Chemicals), doxorubicin (D1515, Sigma), or bleocin (203408, Calbiochem) for 24 or 48 hours as indicated. Assays were performed with the CellTiter-Glo Luminescent Cell Viability Assay Kit according to the manufacturer's instructions (Promega).

Clonogenic survival assays

Cells were seeded in six-well plates (800 or 1500 cells per well) for 24 hours and irradiated with doses as indicated or treated with indicated chemotherapeutic drugs for 24 hours before changing to normal medium. Bleocin-containing medium was then removed and replaced with fresh media. Cells were left for 8 to 12 days until formation of visible colonies. Colonies were washed with PBS, fixed with 10% acetic acid/10% methanol for 20 min, and then stained with 0.4% crystal violet/20% ethanol for 20 min. After staining, the plates were washed with distilled water and air-dried. Afterward, numbers of colonies were counted and analyzed for statistical significance using Excel by Student's *t* tests. The investigators were not blinded to allocation during experiments and outcome assessment.

UV laser–induced DNA damage and immunofluorescence

U2OS cells expressing indicated ubiquitin mutants were treated with doxycycline (1 μg/ml) for 48 hours to induce the depletion of endogenous ubiquitin and expression of exogenous ubiquitin mutants. Cells sensitized to UV-A laser by preincubation with 10 μM 5-bromo-2′-deoxyuridine for 12 hours were microirradiated using a PALM MicroBeam with fluorescence illumination (Zeiss) at ~40 to 46% laser energy and 40% speed (λ = 355 nM). Cell-by-cell microirradiation was carried out, and irradiated cells were recovered for 30 min before fixation with 3.7% formaldehyde. Subsequent immunofluorescence was performed as described above.

Yeast strains and plasmid shuffle assays

The yeast strains used and their pertinent characteristics are provided in table S2. The yeast strain SUB592 (*54*), also named JSY171, was engineered with all ubiquitin genes deleted and a 6×His-myc-ubiquitin-coding plasmid introduced. pUB39 plasmids expressing wild type, T9A, T14A, or E34A yeast synthetic ubiquitin were introduced into SUB592 using standard yeast LiOAc transformation protocol. The resulting strains were selected on CM-LYS plates and subsequently plated on 5-fluoroorotic acid plates for standard plasmid shuffle assays to eliminate the cells expressing wild-type ubiquitin with uracil auxotrophy 3 (*ura3*) markers. Survived cells were grown at 30°C to log phase (optical density at 600 nm, 1 to 1.5), and standard 1:10 series dilution assays were performed in the YPD medium plates with the indicated drugs. Ubiquitin expressed from the *CUP1* promoter was induced by the addition of 100 μM $CuSO_4$.

For drug sensitivity assays using yeast strains expressing various ubiquitin Lys to Arg mutants, we used two ubiquitin expressing constructs in each strain: a wild-type ubiquitin plasmid induced by the galactose-inducible *GAL10* promoter and a mutant ubiquitin plasmid induced by the constitutive *CUP1* promoter. Thus, in YPD media containing galactose, both wild-type and mutant ubiquitin were actively expressed, and switching to glucose-containing media eliminated the expression of the wild-type but not mutant ubiquitin.

SUPPLEMENTARY MATERIALS

www.sciencesignaling.org/cgi/content/full/11/533/eaar8133/DC1

Fig. S1. K63-linked polyubiquitin chains bind free and nucleosomal DNA in vitro.

Fig. S2. K63-linked polyubiquitin chains bind DNA through a newly identified DIP motif including Thr^{9}, Lys^{11}, and Glu^{34} residues.

Fig. S3. Binding to DNA does not disrupt but rather facilitate K63-linked polyubiquitin chains in binding proteins.

Fig. S4. Deficiency in binding DNA leads to attenuated ability for K63-linked polyubiquitin chains in facilitating DDR.

Fig. S5. Cancer patient–derived ubiquitin mutants in the DIP motif display attenuated ability in repairing damaged DNA in part due to deficiency in binding DNA.

Table S1. Oligonucleotides.

Table S2. Yeast strains used in this study.

Reference (*56*)

REFERENCES AND NOTES

1. F. Al-Ejeh, R. Kumar, A. Wiegmans, S. R. Lakhani, M. P. Brown, K. K. Khanna, Harnessing the complexity of DNA-damage response pathways to improve cancer treatment outcomes. *Oncogene* **29**, 6085–6098 (2010).
2. C. F. M. Menck, V. Munford, DNA repair diseases: What do they tell us about cancer and aging? *Genet. Mol. Biol.* **37**, 220–233 (2014).
3. A. Ciccia, S. J. Elledge, The DNA damage response: Making it safe to play with knives. *Mol. Cell* **40**, 179–204 (2010).
4. J. W. Harper, S. J. Elledge, The DNA damage response: Ten years after. *Mol. Cell* **28**, 739–745 (2007).
5. B.-B. S. Zhou, S. J. Elledge, The DNA damage response: Putting checkpoints in perspective. *Nature* **408**, 433–439 (2000).
6. M. S. Y. Huen, R. Grant, I. Manke, K. Minn, X. Yu, M. B. Yaffe, J. Chen, RNF8 transduces the DNA-damage signal via histone ubiquitylation and checkpoint protein assembly. *Cell* **131**, 901–914 (2007).
7. N. K. Kolas, J. R. Chapman, S. Nakada, J. Ylanko, R. Chahwan, F. D. Sweeney, S. Panier, M. Mendez, J. Wildenhain, T. M. Thomson, L. Pelletier, S. P. Jackson, D. Durocher, Orchestration of the DNA-damage response by the RNF8 ubiquitin ligase. *Science* **318**, 1637–1640 (2007).
8. B. Sobhian, G. Shao, D. R. Lilli, A. C. Culhane, L. A. Moreau, B. Xia, D. M. Livingston, R. A. Greenberg, RAP80 targets BRCA1 to specific ubiquitin structures at DNA damage sites. *Science* **316**, 1198–1202 (2007).
9. A. Fradet-Turcotte, M. D. Canny, C. Escribano-Díaz, A. Orthwein, C. C. Y. Leung, H. Huang, M.-C. Landry, J. Kitevski-LeBlanc, S. M. Noordermeer, F. Sicheri, D. Durocher, 53BP1 is a reader of the DNA-damage-induced H2A Lys 15 ubiquitin mark. *Nature* **499**, 50–54 (2013).
10. G. S. Stewart, S. Panier, K. E. B. Townsend, A. K. Al-Hakim, N. K. Kolas, E. S. Miller, S. Nakada, J. Ylanko, S. Olivarius, M. Mendez, C. E. Oldreive, J. Wildenhain, A. Tagliaferro, L. Pelletier, N. Taubenheim, A. H. Durandy, P. J. Byrd, T. Stankovic, A. M. R. Taylor, D. Durocher, The RIDDLE syndrome protein mediates a ubiquitin-dependent signaling cascade at sites of DNA damage. *Cell* **136**, 420–434 (2009).
11. D. Komander, M. Rape, The ubiquitin code. *Annu. Rev. Biochem.* **81**, 203–229 (2012).
12. N. Zhang, Q. Wang, A. Ehlinger, L. Randles, J. W. Lary, Y. Kang, A. Haririnia, A. J. Storaska, J. L. Cole, D. Fushman, K. J. Walters, Structure of the s5a:k48-linked diubiquitin complex and its interactions with rpn13. *Mol. Cell* **35**, 280–290 (2009).
13. A. Bremm, S. M. V. Freund, D. Komander, Lys11-linked ubiquitin chains adopt compact conformations and are preferentially hydrolyzed by the deubiquitinase Cezanne. *Nat. Struct. Mol. Biol.* **17**, 939–947 (2010).
14. Y. Kulathu, D. Komander, Atypical ubiquitylation—The unexplored world of polyubiquitin beyond Lys48 and Lys63 linkages. *Nat. Rev. Mol. Cell Biol.* **13**, 508–523 (2012).
15. M. A. Michel, P. R. Elliott, K. N. Swatek, M. Simicek, J. N. Pruneda, J. L. Wagstaff, S. M. V. Freund, D. Komander, Assembly and specific recognition of k29- and k33-linked polyubiquitin. *Mol. Cell* **58**, 95–109 (2015).
16. Y. A. Kristariyanto, S. A. Abdul Rehman, D. G. Campbell, N. A. Morrice, C. Johnson, R. Toth, Y. Kulathu, K29-selective ubiquitin binding domain reveals structural basis of specificity and heterotypic nature of k29 polyubiquitin. *Mol. Cell* **58**, 83–94 (2015).
17. N. Sekiyama, J. Jee, S. Isogai, K.-i. Akagi, T.-h. Huang, M. Ariyoshi, H. Tochio, M. Shirakawa, NMR analysis of Lys63-linked polyubiquitin recognition by the tandem ubiquitin-interacting motifs of Rap80. *J. Biomol. NMR* **52**, 339–350 (2012).
18. B. Shiotani, L. Zou, Single-stranded DNA orchestrates an ATM-to-ATR switch at DNA breaks. *Mol. Cell* **33**, 547–558 (2009).
19. G. Gill, SUMO and ubiquitin in the nucleus: Different functions, similar mechanisms? *Genes Dev.* **18**, 2046–2059 (2004).
20. Y. Sato, A. Yoshikawa, H. Mimura, M. Yamashita, A. Yamagata, S. Fukai, Structural basis for specific recognition of Lys 63-linked polyubiquitin chains by tandem UIMs of RAP80. *EMBO J.* **28**, 2461–2468 (2009).

21. A.-X. Song, C.-J. Zhou, Y. Peng, X.-C. Gao, Z.-R. Zhou, Q.-S. Fu, J. Hong, D.-H. Lin, H.-Y. Hu, Structural transformation of the tandem ubiquitin-interacting motifs in ataxin-3 and their cooperative interactions with ubiquitin chains. *PLOS ONE* **5**, e13202 (2010).
22. A. K. L. Leung, Poly(ADP-ribose): An organizer of cellular architecture. *J. Cell Biol.* **205**, 613–619 (2014).
23. J. H. Hurley, S. Lee, G. Prag, Ubiquitin-binding domains. *Biochem. J.* **399**, 361–372 (2006).
24. Z.-P. Xia, L. Sun, X. Chen, G. Pineda, X. Jiang, A. Adhikari, W. Zeng, Z. J. Chen, Direct activation of protein kinases by unanchored polyubiquitin chains. *Nature* **461**, 114–119 (2009).
25. W.-L. Yang, J. Wang, C.-H. Chan, S.-W. Lee, A. D. Campos, B. Lamothe, L. Hur, B. C. Grabiner, X. Lin, B. G. Darnay, H.-K. Lin, The E3 ligase TRAF6 regulates Akt ubiquitination and activation. *Science* **325**, 1134–1138 (2009).
26. L. Deng, C. Wang, E. B. Spencer, L. Yang, A. E. Braun, J. You, C. A. Slaughter, C. M. Pickart, Z. Chen, Activation of the IκB kinase complex by TRAF6 requires a dimeric ubiquitin-conjugating enzyme complex and a unique polyubiquitin chain. *Cell* **103**, 351–361 (2000).
27. T. E. Messick, R. A. Greenberg, The ubiquitin landscape at DNA double-strand breaks. *J. Cell Biol.* **187**, 319–326 (2009).
28. S. D. Weeks, K. C. Grasty, L. Hernandez-Cuebas, P. J. Loll, Crystal structures of Lys-63-linked tri- and di-ubiquitin reveal a highly extended chain architecture. *Proteins* **77**, 753–759 (2009).
29. I. Dikic, S. Wakatsuki, K. J. Walters, Ubiquitin-binding domains—From structures to functions. *Nat. Rev. Mol. Cell Biol.* **10**, 659–671 (2009).
30. L. Jin, A. Williamson, S. Banerjee, I. Philipp, M. Rape, Mechanism of ubiquitin-chain formation by the human anaphase-promoting complex. *Cell* **133**, 653–665 (2008).
31. L. Bedford, J. Lowe, L. R. Dick, R. J. Mayer, J. E. Brownell, Ubiquitin-like protein conjugation and the ubiquitin–proteasome system as drug targets. *Nat. Rev. Drug Discov.* **10**, 29–46 (2011).
32. R. I. Enchev, B. A. Schulman, M. Peter, Protein neddylation: Beyond cullin–RING ligases. *Nat. Rev. Mol. Cell Biol.* **16**, 30–44 (2015).
33. H. Kim, J. Chen, X. Yu, Ubiquitin-binding protein RAP80 mediates BRCA1-dependent DNA damage response. *Science* **316**, 1202–1205 (2007).
34. B. Wang, S. Matsuoka, B. A. Ballif, D. Zhang, A. Smogorzewska, S. P. Gygi, S. J. Elledge, Abraxas and RAP80 form a BRCA1 protein complex required for the DNA damage response. *Science* **316**, 1194–1198 (2007).
35. J. Spence, S. Sadis, A. L. Haas, D. Finley, A ubiquitin mutant with specific defects in DNA repair and multiubiquitination. *Mol. Cell. Biol.* **15**, 1265–1273 (1995).
36. S. P. Jackson, D. Durocher, Regulation of DNA damage responses by ubiquitin and SUMO. *Mol. Cell* **49**, 795–807 (2013).
37. W. Zhang, Z. Qin, X. Zhang, W. Xiao, Roles of sequential ubiquitination of PCNA in DNA-damage tolerance. *FEBS Lett.* **585**, 2786–2794 (2011).
38. C. M. Kondratick, E. M. Boehm, L. M. Dieckman, K. T. Powers, J. C. Sanchez, S. R. Mueting, M. T. Washington, Identification of new mutations at the PCNA subunit interface that block translesion synthesis. *PLOS ONE* **11**, e0157023 (2016).
39. M. Xu, B. Skaug, W. Zeng, Z. J. Chen, A ubiquitin replacement strategy in human cells reveals distinct mechanisms of IKK activation by TNFα and IL-1β. *Mol. Cell* **36**, 302–314 (2009).
40. J. Condeelis, R. H. Singer, J. E. Segall, The great escape: When cancer cells hijack the genes for chemotaxis and motility. *Annu. Rev. Cell Dev. Biol.* **21**, 695–718 (2005).
41. A. L. Haas, K. D. Wilkinson, DeTEKting ubiquitination of APC/C substrates. *Cell* **133**, 570–572 (2008).
42. A. Plechanovová, E. G. Jaffray, M. H. Tatham, J. H. Naismith, R. T. Hay, Structure of a RING E3 ligase and ubiquitin-loaded E2 primed for catalysis. *Nature* **489**, 115–120 (2012).
43. P. S. Brzovic, A. V. Lissounov, D. E. Christensen, D. W. Hoyt, R. E. Klevit, A UbcH5/ubiquitin noncovalent complex is required for processive BRCA1-directed ubiquitination. *Mol. Cell* **21**, 873–880 (2006).
44. Y. Zhao, J. R. Brickner, M. C. Majid, N. Mosammaparast, Crosstalk between ubiquitin and other post-translational modifications on chromatin during double-strand break repair. *Trends Cell. Biol.* **24**, 426–434 (2014).
45. C. Wang, L. Deng, M. Hong, G. R. Akkaraju, J.-i. Inoue, Z. J. Chen, TAK1 is a ubiquitin-dependent kinase of MKK and IKK. *Nature* **412**, 346–351 (2001).
46. S. Liu, J. Chen, X. Cai, J. Wu, X. Chen, Y.-T. Wu, L. Sun, Z. J. Chen, MAVS recruits multiple ubiquitin E3 ligases to activate antiviral signaling cascades. *eLife* **2**, e00785 (2013).
47. A. Flotho, F. Melchior, Sumoylation: A regulatory protein modification in health and disease. *Annu. Rev. Biochem.* **82**, 357–385 (2013).
48. D. Gao, H. Inuzuka, A. Tseng, R. Y. Chin, A. Toker, W. Wei, Phosphorylation by Akt1 promotes cytoplasmic localization of Skp2 and impairs APCCdh1-mediated Skp2 destruction. *Nat. Cell Biol.* **11**, 397–408 (2009).
49. P. Liu, M. Begley, W. Michowski, H. Inuzuka, M. Ginzberg, D. Gao, P. Tsou, W. Gan, A. Papa, B. M. Kim, L. Wan, A. Singh, B. Zhai, M. Yuan, Z. Wang, S. P. Gygi, T. H. Lee, K. -P. Lu, A. Toker, P. P. Pandolfi, J. M. Asara, M. W. Kirschner, P. Sicinski, L. Cantley, W. Wei, Cell-cycle-regulated activation of Akt kinase by phosphorylation at its carboxyl terminus. *Nature* **508**, 541–545 (2014).
50. H. Inuzuka, D. Gao, L. W. S. Finley, W. Yang, L. Wan, H. Fukushima, Y. R. Chin, B. Zhai, S. Shaik, A. W. Lau, Z. Wang, S. P. Gygi, K. Nakayama, J. Teruya-Feldstein, A. Toker, M. C. Haigis, P. P. Pandolfi, W. Wei, Acetylation-dependent regulation of Skp2 function. *Cell* **150**, 179–193 (2012).
51. L. Wan, M. Tan, J. Yang, H. Inuzuka, X. Dai, T. Wu, J. Liu, S. Shaik, G. Chen, J. Deng, M. Malumbres, A. Letai, M. W. Kirschner, Y. Sun, W. Wei, APC^{Cdc20} suppresses apoptosis through targeting Bim for ubiquitination and destruction. *Dev. Cell* **29**, 377–391 (2014).
52. Y. R. Chin, X. Yuan, S. P. Balk, A. Toker, PTEN-deficient tumors depend on AKT2 for maintenance and survival. *Cancer Discov.* **4**, 942–955 (2014).
53. P. Liu, W. Gan, C. Guo, A. Xie, D. Gao, J. Guo, J. Zhang, N. Willis, A. Su, J. M. Asara, R. Scully, W. Wei, Akt-mediated phosphorylation of XLF impairs non-homologous end-joining DNA repair. *Mol. Cell* **57**, 648–661 (2015).
54. J. Spence, R. R. Gali, G. Dittmar, F. Sherman, M. Karin, D. Finley, Cell cycle–regulated modification of the ribosome by a variant multiubiquitin chain. *Cell* **102**, 67–76 (2000).
55. N. Narayana, M. A. Weiss, Crystallographic analysis of a sex-specific enhancer element: Sequence-dependent DNA structure, hydration, and dynamics. *J. Mol. Biol.* **385**, 469–490 (2009).
56. P. Xu, D. M. Duong, N. T. Seyfried, D. Cheng, Y. Xie, J. Robert, J. Rush, M. Hochstrasser, D. Finley, J. Peng, Quantitative proteomics reveals the function of unconventional ubiquitin chains in proteasomal degradation. *Cell* **137**, 133–145 (2009).

Acknowledgments: We thank S. J. Elledge (Harvard University), A. E. Elia (Harvard University), W. Harper (Harvard University), W. Johannes (Harvard University), D. J. Finley (Harvard University), H. Wu (Harvard University), and Z. J. Chen [University of Texas Southwestern Medical Center (UT Southwestern)] for insightful suggestions and critiques. We also thank B. North (Beth Israel Deaconess Medical Center), as well as Wei and Liu laboratory members, for critical reading of the manuscript, and members of the Wei, Liu, Elledge, and Wu laboratories for helpful discussions. We thank X. Tan (University of North Carolina at Chapel Hill) for evaluation of all statistical analyses. We thank D. Komander (MRC Laboratory of Molecular Biology), J. Peng (Emory University), T. M. Washington (University of Iowa), D. J. Finley (Harvard University), and Z. J. Chen (UT Southwestern) for sharing the valuable ubiquitin chains, critical yeast strains, and mammalian ubiquitin depletion cell lines. We also thank F. Lan and S. Yang for sharing the valuable recombinant nucleosomes and histone octamers and Y. Xiang for sharing the HeLa nuclear extracts. We thank G. Gupta for sharing the the Flag-HA-BRCA1 plasmid. **Funding:** W.W. is a Leukemia and Lymphoma Society scholar. W.G. is supported by K99CA207867 from the National Cancer Institute. This work was supported in part by the NIH grants [R01CA177910 (W.W.) and R01GM094777 and R00CA181342 (P.L.)]. **Author contributions:** P.L., W.G., A.V.H., T.-m.F., B.B., and W.W. designed the experiments. P.L., W.G., A.V.H., T.-m.F., C.S., M.X., and A.C.L. performed the experiments and analyzed the data. P.L., W.G., and W.W. wrote the manuscript. All authors commented on the manuscript. P.L. and W.W. supervised the study. **Competing interests:** The authors declare that they have no competing interests. **Data and materials availability:** All data needed to evaluate the conclusions in the paper are present in the paper and/or the Supplementary Materials. Plasmids are available upon request.

Submitted 20 December 2017
Accepted 16 May 2018
Published 5 June 2018
10.1126/scisignal.aar8133

Citation: P. Liu, W. Gan, S. Su, A. V. Hauenstein, T.-m. Fu, B. Brasher, C. Schwerdtfeger, A. C. Liang, M. Xu, W. Wei, K63-linked polyubiquitin chains bind to DNA to facilitate DNA damage repair. *Sci. Signal.* **11**, eaar8133 (2018).

K63-linked polyubiquitin chains bind to DNA to facilitate DNA damage repair

Pengda Liu, Wenjian Gan, Siyuan Su, Arthur V. Hauenstein, Tian-min Fu, Bradley Brasher, Carsten Schwerdtfeger, Anthony C. Liang, Ming Xu and Wenyi Wei

Sci. Signal. **11** (533), eaar8133.
DOI: 10.1126/scisignal.aar8133

DNA-bound ubiquitin coordinates DNA repair

Ubiquitylation is a posttranslational modification that reversibly alters protein stability, activity, interactions, or trafficking. The ubiquitylation of histones and various other proteins facilitates the response to DNA damage. However, Liu *et al.* discovered that ubiquitin also binds directly to DNA. In solution and in live cells, chains of ubiquitin specifically linked through Lys^{63} residues (referred to as K63-linked polyubiquitin chains) preferentially bound to the free ends of double-stranded DNA through a three-amino acid motif in ubiquitin that the authors call a "DNA-interacting patch" (DIP). These chains appeared to bind the broken ends of DNA and recruit repair proteins. Ubiquitins with mutations in the DIP were found in several types of tumors and, when expressed in cultured cells, impaired the cellular response to DNA-damaging agents, suggesting that these mutations might be exploited for therapeutic benefit in some cancer patients.